Large-scale brain signatures of fluid dynamics and responsiveness linked to consciousness

M. Breyton[1], J. Fousek[1], G. Rabuffo[1], P. Sorrentino[1], L. Kusch[1], M.Massimini[2], S. Petkoski[1], V. Jirsa[1]
[1]Aix Marseille Université, 13005 Marseille, France, Inserm, Institut Neurosciences Systèmes, Umr 1106, Marseille, France
[2]University of Milan

Abstract:

Neural bases of consciousness have been explored through many different paradigms and the notion of complexity emerged as a unifying framework to characterize conscious experience. To date, the perturbational complexity index (PCI), rooted on information theory, shows high performance in assessing consciousness. However, the mechanisms underpinning this perturbational complexity remain unclear as well as its counterpart in spontaneous activity. In the present study, we explore brain responsiveness and resting-state activity through large-scale brain modeling and prove that complexity and consciousness are directly associated with a fluid dynamical regime. This fluidity is reflected in the dynamic functional connectivity, and other metrics drawn from dynamical systems theory and manifolds can capture such dynamics in synthetic data. We then validate our findings on a cohort of 15 subjects under anesthesia and wakefulness and show that measures of fluidity on spontaneous activity can distinguish consciousness in agreement with perturbational complexity.

1. Introduction:

The human brain is among the most complex systems known in nature. Brain function ranges from simple information processing operations to complex behavior, cognition and up to phenomenological conscious experience. A striking feature of the brain is the ability to operate in different dynamical regimes allowing for flexible switches between functional states as well as stable and sustained activity. Unveiling the organizational principles and mechanisms giving rise to such diverse behavior is still an open question in science. Wakefulness is generally associated with consciousness, a state where the brain can dynamically adapt to a wide range of stimuli, which typically present themselves in a noisy, ever-changing environment. On the contrary, other dynamical regimes are not compatible with such flexibility, and in some cases the subject can appear unresponsive to an external observer. For example, during sleep there are at least 5 stages, each with a characteristic organization of large-scale neuronal activity (Attarian et Undevia 2012), and a corresponding degree of consciousness. During rapid eye movement (REM) sleep, subjects are unresponsive

but are likely to report dreaming experience (Hobson 2009). Thus, REM sleep is generally associated with a mildly stable dynamical regime and disconnected consciousness. However, non-rapid eye movement sleep early in the night (NREM3) is a more stable state from which it is harder to be awakened and is rarely associated with consciousness (Patel et al. 2022). Similar to sleep, anesthesia (Fig 1.a) can be used to medically trigger comatose states of various depths associated with unresponsiveness. Typical anesthetic drugs like Xenon or Propofol induce a state resembling NREM sleep (Murphy et al. 2011). Others, like Ketamine can induce an unresponsive yet active state much like REM sleep. The idea that consciousness is not discrete, but there rather exists a "gradient" of consciousness poses a great challenge to physicians dealing with unresponsive patients. In this context, detecting consciousness in brain injured patients with poor behavioral output can be very challenging. In an attempt to solve this problem, recent studies have developed a technique based on transcranial magnetic stimulation (TMS, Casali et al. 2013). In brief, the brain is magnetically (Hallett 2007) perturbed (non-invasively), and the subsequent relaxation of the system is recorded with electroencephalography (EEG). It has been demonstrated that the post-stimulus response can be qualitatively different depending on the state of the patient (awake, REM, anesthesia, etc.), and quantitatively measured by a simple scalar: the perturbational complexity index (PCI). The PCI accounts for the complexity of the distributed spatiotemporal response in the brain, with values close to 1 when the complexity is high, and closer to 0 for simpler responses. Notably, growing evidence points at the PCI index as a reliable marker (Fig 1.b) to discriminate between awake subjects and subjects in NREM sleep or in an anesthetic-induced coma (Casarotto et al. 2016; Sarasso et al. 2015).

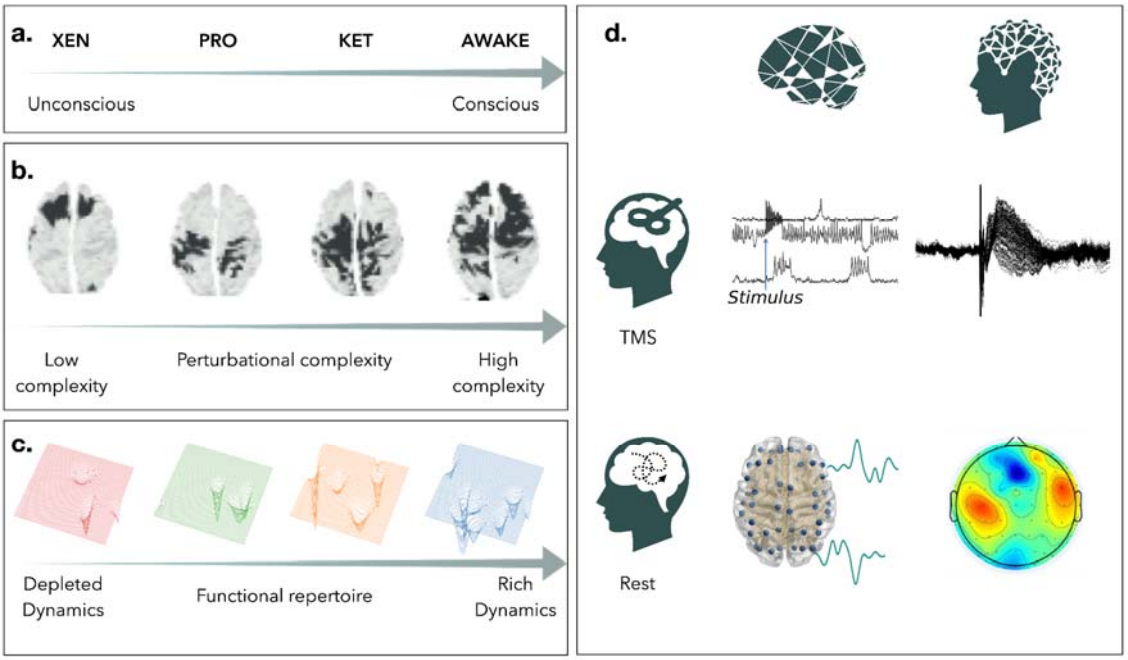

Fig 1: Conceptual framework of the study

(a) Consciousness is a continuum and can be explored with drug-induced coma of various depths (Xenon, Propofol > Ketamine > Wakefulness). We hypothesized a correspondence between the variations in complexity found with PCI and the dynamics of spontaneous

activity across the spectrum of consciousness. (b) We sketched various patterns of spatio-temporal activity reflecting changes in perturbational complexity from left to right. In (c) we showed the conceptual shapes of corresponding manifolds of brain activity responsible for different sizes of the functional repertoire (number of wells) and associated with consciousness. (d) The brain is modeled as a network of neural masses coupled by an empirical connectome. This whole-brain model serves as a platform to simulate resting state activity (bottom left) and cortical stimulation (top left, example of firing rate time series with applied stimulus). Dynamical properties of the simulations are studied and compared with data features of human empirical recordings of spontaneous activity (bottom right, EEG during wakefulness and under three anesthetics) and stimulation (top right, TMS-EEG protocol performed in the same conditions).

Alongside, stability and complexity find solid mathematical definitions in the context of dynamical system theory. Dynamical system theory has gained momentum in neuroscience to study the evolution of spontaneous resting state activity, i.e. *resting state*. In fact, resting-state activity is highly organized, and structured patterns of regional activations are observed in large-scale recordings, across imaging modalities. Some of these co-activation patterns have been found to be so stable across individuals that they were identified as functional brain networks (Damoiseaux et al. 2006). When unfolded in time, such activation patterns can form and recur over several seconds of recording, hinting at a rich temporal structure. The typical topographic organization of activity patterns is captured by Functional Connectivity (FC) measures (van den Heuvel et Hulshoff Pol 2010; Greicius 2008; Fox et Greicius 2010) which are static views of the functional coordination between brain regions. These patterns however are also continuously changing over time. The temporal organization is estimated by dynamic Functional Connectivity (dFC) measures, for example by correlating FC patterns at distinct time windows (Preti, Bolton, et Van De Ville 2017; Hansen et al. 2015). In this paradigm, data complexity can be associated with the variety of activity patterns explored in time (Ghosh et al. 2008; Jirsa et Sheheitli 2022) defining a functional repertoire (Fig 1.c). As said earlier, only specific dynamical regimes are capable of supporting complex dynamics, i.e. explore a high number of states (Hansen et al. 2015).

In this work, we aimed at exploring the relationship between perturbational complexity and the richness of the functional repertoire, as conceptualized above. For that purpose, we leveraged the *in silico* framework provided by The Virtual Brain (TVB) (Sanz Leon et al. 2013) to build a large-scale brain network model and simulate non-invasive brain stimulation in a range of distinct dynamical regimes (Fig 1. d). In large-scale brain models, the cortex is parcellated in brain regions, each modeled by a neural mass model (Deco et al. 2008). The neural masses are coupled through the anatomical connectivity, i.e. the connectome, which contains the number of white matter tracts connecting brain regions, along with their length (Sporns 2011).

Much evidence converges towards a conceptualization of the brain as self-regulating around a special regime of activity laying between and ordered and a disorder phase (Cocchi et al. 2017; O'Byrne et Jerbi 2022). The computational model of the brain that we employed allowed us to explore this transition by varying a global coupling parameter that scales the

influence of the structural connections as compared to the local regional dynamics. Previous work has shown that, when the global coupling parameter is properly scaled, the *in-silico* system can produce phenomena of co-activations between brain regions, giving rise to realistic FC patterns and non-trivial dFC, as observed empirically in fMRI experiments (Rabuffo et al. 2021). Here, we quantify the response to simulated TMS across dynamical regimes (as defined by the global coupling) using the simulation PCI (sPCI) and link it to dFC metrics. Our hypothesis is that in-silico simulations can only yield high sPCI and non-trivial dFC when the system is fine-tuned in a specific regime. We then validate our results by comparing empirical spontaneous and stimulation data of 15 subjects, each acquired during wakefulness and during different states of consciousness (Propofol anesthesia (N=5), Xenon anesthesia (N=5), Ketamine anesthesia (N=5)).

2. Results:

2.1. Large-scale brain model and dynamical regimes

To explore the relationship between resting state dynamics and brain responsiveness, we built a large-scale brain network model (Sanz Leon et al. 2013), consisting of 84 cortical and subcortical regions. Each of them is conceptualized by a neural mass model (NMM) made of a set of stochastic nonlinear differential equations, which describes the evolution of the mean firing rate r(t) and mean membrane potential V(t) of an ensemble of quadratic integrate and fire (QIF) neurons (Montbrió, Pazó, et Roxin 2015). The equations ascribe the dynamics of the NMM to two fixed points corresponding to an oscillatory, high-firing *upstate* (inward spiral) and a low-firing *downstate* (stable fixed point). Each node is driven by a stochastic noise component, which for high magnitude values pushes the activity towards the upstate and vice versa. When plugged into a brain network, the state of each NMM is also dictated by the input from its neighbors through the connectome. The input from any region is weighted by the size of the bundle of white fiber tracts estimated by diffusion weighted imaging (DWI). Here, we use a generic connectome of one healthy subject from the human connectome project (HCP, (Van Essen et al. 2013). At the network level, spontaneous activity can show a variety of dynamics depending on two global parameters: the global coupling G (which scales the connectome) and noise intensity σ (white noise with zero mean and standard deviation σ) (Fig 2.a). In the *low coupling* regime (Fig 2.a, left side), regions of the network are weakly connected and mostly behave independently, driven by noise input alone. Hence, when the noise is low (Fig 2.a, bottom left corner), the activity is generally low and sparse, as most of the nodes are in the down state, with some rare and transient activations. As noise increases (Fig 2.a, top left corner), activations are more frequent, yet stochastic and non-coherent. When global coupling is set to a high value (Fig 2.a, right side), brain regions are tightly connected, and the activity of each node is heavily entrained by the rest of the network. In this setting, most nodes tend to stay in the upstate due to high average input (proportional to G, since $I(t) = f(G, W)$). Only nodes that are weakly connected to the rest of the network will stay in the downstate despite high coupling. This behavior gives rise to a stable pattern of regional coactivations that involve characteristic subnetwork mirroring the structural connectivity (Rabuffo et al. 2021; Pope et al. 2021) and resulting in stereotyped activity on a

slow timescale. However, in-between these two regimes, there exists an intermediate *working point* (Fig 2.a, middle) where cascades of coactivations of different sizes and durations occur in a complex fashion, and the system becomes more unpredictable. Yet these patterns of coactivations are not random (Battaglia et al. 2020) and can occur multiple times, which is interpreted as the system visiting the same neighborhood of its manifold multiple times.

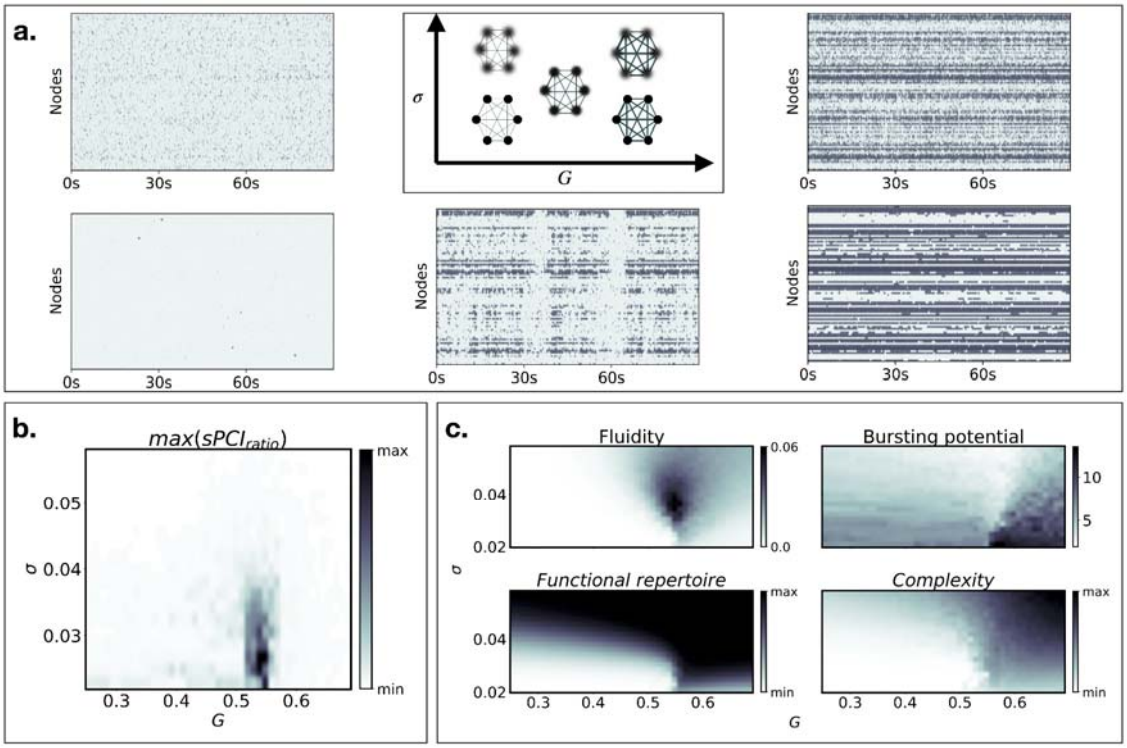

Fig 2: Dynamical regimes and associated metrics

(a) Examples of firing rate times series of the model depending on the strength of interaction between nodes (global coupling, G) and noise intensity (sigma). On the left column, the interactions are weak (G=0.27, sigma-bottom=0.022, sigma-top=0.056) and the activity is sparse. On the right column, connections are tighter (G=0.65, sigma-bottom=0.022, sigma-top=0.056) and a stable coactivation pattern appears in an ordered fashion. In the middle (bottom) global coupling and noise are at optimal values (G=0.56, sigma=0.036) and allow the emergence of structured patterns (coactivation cascades) of different sizes and durations. (b) Analysis of in-silico stimulation revealed that the same dynamical regime around the optimal point reaches the highest change in complexity (color scale: max(sPCI ratio) in parameter space G, sigma). (c) Results of the four resting state metrics that we studied across dynamical regimes i.e in the parameter space of the model. (c, top left) results of the fluidity of the spontaneous firing rate activity (Variance(dFC) with a sliding window of 3s and 1s step-size). In (c, top right) we show the results of bursting potential assessed by the fastest change in the residual sum of squares across sources' membrane potential. (c, bottom left) presents the size of the functional repertoire defined by the number of unique configurations of binarized firing rate activity (with a threshold at r=0.7). (c, bottom right) Lempel-Ziv complexity of binarized firing rate activity (with a threshold at r=0.7).

2.2. Modeling stimulation and spontaneous activity

Brain stimulation was modeled by adding a transient external current to the membrane potential, mimicking a single pulse stimulus to a cortical brain region. In line with the experimental protocol, we sampled each regime (i.e., each {G, sigma}) multiple times, varying the initial conditions and stimulating a random selection of 17 cortical nodes. When perturbed, the whole system is pushed out of its current state, as the stimulus propagates through the network and the system relaxes to a new stable state. For each simulation, we measured the complexity of the activity over 10 seconds following the stimulus. To this end, we have used a metric inspired by the perturbational complexity index (*simulation PCI*, *sPCI*) to capture the complexity of the relaxation of the system after the perturbation. We then compared it to the complexity of the baseline (i.e. the same simulation in the absence of a stimulus) by a ratio. This was done to quantify the relationship between the current dynamical regime and the capacity of the system to flexibly integrate a perturbation (see Methods for full description). We found that the maximum increase in complexity is reached when global coupling is set around $G = 0.55$, and complexity itself can be increased five-fold with respect to baseline (Fig 2b). The stimulus has little to no effect on global activity when the system operates far from this *working point.* Accordingly, there is no change in complexity. In the supplementary information S1 we present time series after a stimulus in the different regimes. The Figure shows that stimulation can trigger (or disrupt) a coactivation cascade near the optimal *working point*, but not in other regimes. If the complexity ratio of is greater than one (lower than one) the trajectory of the system was pushed towards (away from) an attractor. The minimum ratio is also shown (supplementary figure S2): one can see that it follows the same distribution as the maximum ratio in the parameter space, reflecting the simulations where a cascade was interrupted by the stimulus. When the ratio is close to one, either there are no stable attractors on the manifold, or it is impossible to move away from the attractor and it's not possible to elicit a response which is more complex than the baseline activity.

To compare responsiveness with resting state activity we extracted the *fluidity* of the system, defined by the variance of the upper triangular part of the dFC. *Fluidity* captures the recurring patterns of co-activation across time and, more specifically, the switches between highly correlated patterns and non-correlated patterns. Though lacking hard evidence due to the difficulty of exploring the manifold of brain activity in humans, fluidity is expected to reflect the complexity of the energy landscape and the number of attractors (Hansen et al. 2015; Fousek et al. 2022). The distribution of *fluidity* in the parameter space (Fig 1c first panel) of the model reveals a peak around the value of the *working point*, reflecting recurring cascades during the simulation, and decreases monotonously as the regime is drawn away from it.

Three additional spontaneous activity metrics are presented. We first calculated the raw Lempel-Ziv (LZ) complexity of each regime after binarization of the time series. LZ complexity counts the number of unique patterns (sequences of bits) found in a binary string, allowing for patterns of different sizes. A simple fixed threshold was used to binarize each time series into a sequence of upstates and downstates. LZ complexity is found to increase abruptly as global coupling crosses the working point separating a low complexity-low coupling regime from a high complexity-high coupling regime. Second, we extracted the size

of the functional repertoire of the model, by counting the number of unique configurations that neuronal avalanches take over time. As for LZ complexity, there is a separation of the space around the working point by a sharp increase of the functional repertoire, although this separation shifts towards lower coupling when noise increases and is lost for regimes with high noise. Lastly, we measured the bursting potential of the system. Bursting potential aims at capturing the fastest change in global activity of the network and it is computed as the maximum of the gradient of the residual sum of squares between sources (see Methods). Again, a similar pattern is seen with an increase around the working point. These tight relationships between simulation features (on spontaneous and stimulated activity) and the tuning of global coupling suggest that the same dynamical regime might underpin both optimal brain responsiveness and optimal spontaneous activity. Under the assumption that global coupling models a free parameter in the brain which is subject to change upon internal and/or external states, global dynamical changes should be found for different brain states. Next, we sought to retrace the signatures of these same dynamical regimes in real data in spontaneous EEG recordings during wakefulness and anesthesia.

2.3. Data analysis

In this section we used previously published experimental data, provided by (Sarasso et al. 2015). 15 healthy subjects underwent a TMS-EEG protocol and a spontaneous EEG during anesthesia (Xenon, Propofol, Ketamine) and wakefulness. These anesthetics were posited as empirical models of loss of consciousness. Reports upon awakening were used as a ground truth for conscious experience and it was found that subjects under Xenon or Propofol had no recollection of conscious experience whereas Ketamine induced anesthesia was always associated with reports of consciousness (i.e. dreaming). During the TMS-EEG protocol multiple sessions of stimulation each consisting of multiple trials per stimulation site were performed. A PCI value (across trials average) was obtained for each session and the maximum PCI across sessions was retained. Only the maximum value of PCI for each subject and condition was available to us. A PCI at 0.31 was benchmarked as a threshold for consciousness (Casarotto et al. 2016). As published previously, PCI successfully distinguishes conscious from unconscious states. Complexity measured with PCI is systematically higher during wakefulness than under anesthesia for Xenon and Propofol drugs, but not for Ketamine induced anesthesia which is grouped with wakefulness (PCI > 0.31). Based on modeling results linking perturbational complexity and spontaneous activity metrics to the same underlying dynamical regimes modulated by global coupling, we hypothesized that variations of complexity should also be found at rest and associated with consciousness.

We studied the four resting state metrics described in the previous section and present their association with consciousness. We demonstrate that consciousness is associated with more complex activity at rest. In fact, for all subjects, at least one metric can perfectly distinguish wakefulness from anesthesia. We first extracted *fluidity* of the recordings on a broad band spectrum (highpass filter at 0,5Hz and lowpass at 60Hz). Dynamic functional connectivity was calculated using circular correlation between electrodes with a sliding window approach (1 second window, 100 ms step size). Then, for each subject and recording we used a bootstrap procedure to sample uniformly with replacement 50 segments of 1 minute.

Complexity, the size of the *functional repertoire* and *bursting capacity* was computed on each segment. When binarization was needed, we z-scored each electrode independently and thresholded at 3 standard deviations. This yielded a distribution of 50 points for each subject and condition (anesthesia or wakefulness). We present in Figure 3 the results, subject-wise, for the 4 resting state metrics we studied: *fluidity*, *complexity*, *functional repertoire* and *bursting capacity* between anesthesia and wakefulness conditions. In Figure 4, we show classification results when grouping participants either on anesthesia (vs wakefulness) or conscious report (vs no report). We cross plotted each metrics against the PCI on the top and show classification accuracies of all metrics after fitting an SVM classifier with a linear kernel. For these last results we computed complexity and the size of the functional repertoire on the full recordings and adjusted by the length of the signal.

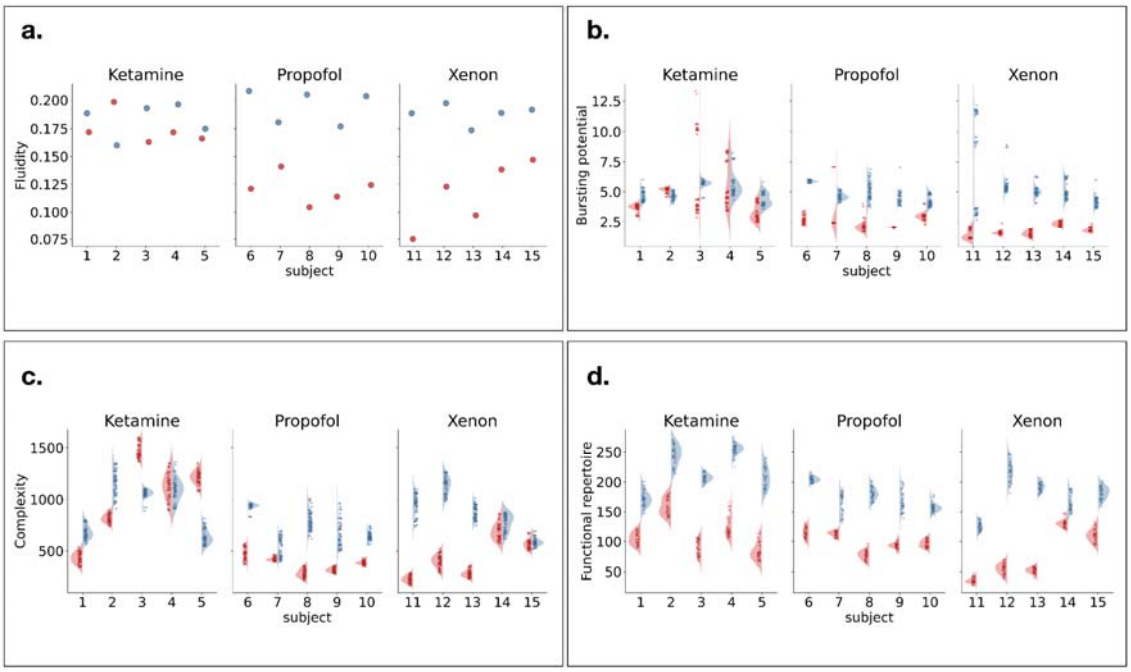

Fig 3: Resting-state metrics on EEG during anesthesia and wakefulness
Subject-specific distributions of (a) fluidity, (b) bursting capacity, (c) Lempel-Ziv complexity and (d) the size of the functional repertoire, between wakefulness (blue) and anesthesia (red). From left to right in each panel : Ketamine group, Propofol group and Xenon group. Values and distributions (kernel density estimations) were obtained by randomly sampling with replacement a minute of signal within each subject's recording (50 samples drawn per subject per condition, 1 point per sample). Fluidity was calculated on the full recordings for each subject.

According to our hypothesis and modeling results, we expected higher values of *fluidity* during wakefulness than anesthesia (Fig 3.a). The separation between conditions was perfect for Propofol and Xenon anesthesia. Ketamine results were inconsistent, with subject 2 showing a reversed pattern (higher fluidity during anesthesia). The classification by conscious report was perfect (100% accuracy), just like with the PCI (Fig 4. top). Based on the results obtained on perturbational complexity, we expected to find systematically more spontaneous complexity during wakefulness than anesthesia (Fig 3.c). For Propofol anesthesia all subjects had a good separation and for Xenon, 3 subjects were well classified but two had overlapping

distributions of complexity. For Ketamine, subject 4 had overlapping distributions when the other 4 showed good separation though the relationship was inverted for subjects 3 and 5 with less complexity found in wakefulness. In line with (Rabuffo et al. 2021), we hypothesized that bursting capacity was associated with the flexibility of the brain to switch between distant functional states and expected this ability to be lost during anesthesia. The results for bursting capacity were satisfying for the Xenon and Propofol conditions but poor for all subjects under Ketamine (Fig 3.b). As expected, when the separation occurs between wakefulness and anesthesia, the bursting potential is consistently higher during wakefulness. It's probably hinting at different mechanisms of action of the drugs on neural dynamics, in which bursting capacity is not altered by Ketamine. Lastly, as the size of the functional repertoire reflects the extent of explored functional patterns, we were expecting to find it associated with wakefulness, when the brain is more solicited and needs to reconfigure more often. Indeed (Fig 3.d), it is the metric that permits a perfect separation between wakefulness and anesthesia for all subjects and conditions. The number of states explored during the recordings was consistently larger during wakefulness than anesthesia for all drugs and subjects.

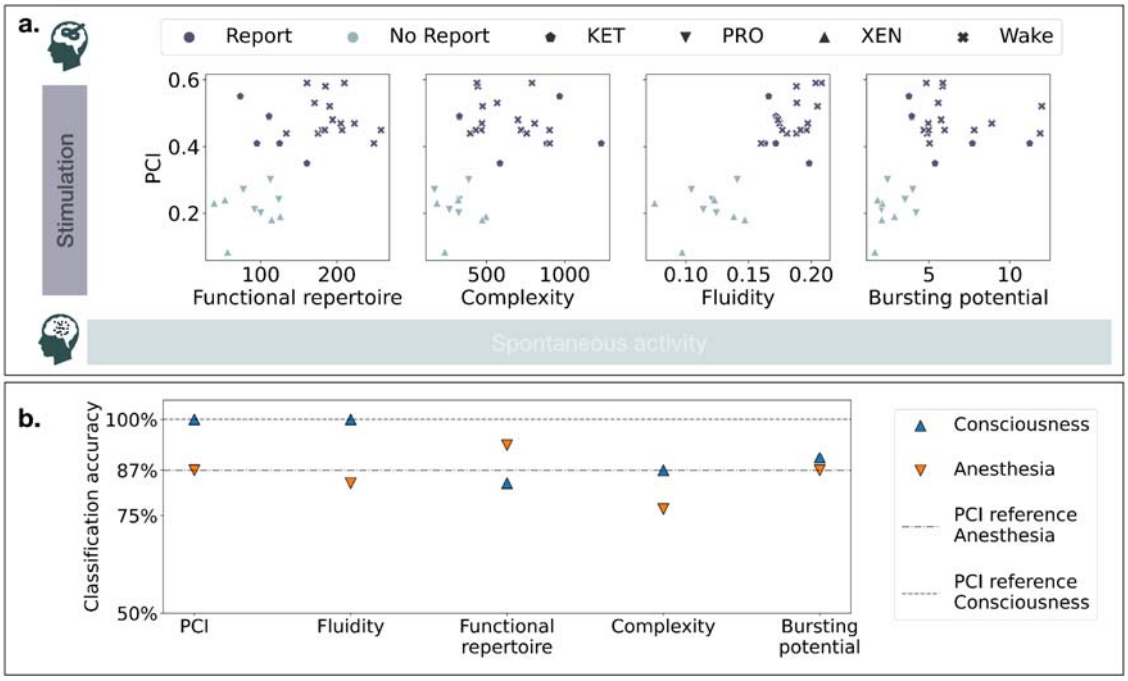

Fig 4: Predictive power of resting-state metrics and PCI

(a) Crossplots between the PCI obtained experimentally during a TMS-EEG protocole and each metric on spontaneous recordings (functional repertoire, complexity, fluidity and bursting potential). Complexity and the size of the functional repertoire were normalized by the length of the recording in minutes. (b) Classification accuracy of a Support Vector Machine classifier with a linear kernel to distinguish either between anesthesia and wakefulness (downward orange triangles) or between conscious report and no report (upward blue triangles). Dashed lines represent the benchmark performances achieved by PCI classification (100% for consciousness and 87% for anesthesia).

3. Discussion:

Understanding the neural substrates of consciousness is one of the greatest scientific problems, both from a philosophical and a theoretical standpoint. This challenge also stems from clinical practice, such as the need to characterize disorders of consciousness and their prognosis (Edlow et al. 2021; Sanders et al. 2012; Giacino et al. 2018). The detection of consciousness independently of sensory processing and motor behavior has recently improved with the development of the Perturbational Complexity Index that relies on the analysis of TMS-evoked potentials (Casarotto et al. 2016). Despite its remarkable performance TMS-EEG can be difficult to implement in clinical practice and it requires complex equipment. In this work, we explored both the dynamics of spontaneous activity and responsiveness in a large-scale brain model and found strong evidence that common network-level factors govern the two. We demonstrate using a large-scale brain model that a similar working point can cause perturbational complexity and complex (fluid) spontaneous activity. We then showed using empirical data that spontaneous activity analyzed through appropriate metrics can be effective in assessing consciousness in wakefulness and anesthesia.

A large body of evidence explores a relationship between the complexity of brain signals and conscious experience, as recently reviewed (Sarasso et al. 2021). The first theoretical argument started from a phenomenological description of conscious experience that led to theorizing the expected properties of the underlying neural activity (Tononi 1998; Tononi et al. 1998). In this view, the two building blocks of consciousness are functional integration (each experience is unified as a whole) and functional differentiation (each experience is unique and separated from others). These theoretical findings lead to the development of metrics rooted in information theory to estimate these functional properties on neural data. Of all these metrics, the PCI (relying on Lempel-Ziv complexity and entropy) revealed an interpretable and practical link between the spatio-temporal complexity of the propagation of a perturbation in the brain and the level of consciousness. In parallel, large literature is dedicated to understanding brain function from the perspective of dynamical systems theory. In this field, the brain is viewed as a complex open system far from equilibrium composed of a large number of coupled components (e.g., neurons at the microscale or neural masses at the mesoscale) whose interactions are responsible for the emergence of macroscopic patterns. In such systems, drastic changes such as phase transitions or bifurcations can occur spontaneously or under the influence of a global parameter, with major effects on the dynamics. Brain simulations like the one presented in this work support the idea that a rich dynamics is possible when the system's parameters are fine-tuned around specific values (Golos, Jirsa, et Daucé 2015). In fact, although debated, one prominent theory in neurosciences posits that the brain self-regulates near a critical regime i.e. in the vicinity of a phase transition (Cocchi et al. 2017; O'Byrne et Jerbi 2022). Simply put, this property allows the brain to be flexible enough to reconfigure and adapt dynamically to a changing environment all while being stable enough to engage in complex sustained activities. Among other things, the critical regime is known to maximize information processing (Beggs 2008) or related to cognitive processes (Xu, Feng, et Yu 2022), and criticality in the brain is also possibly linked to consciousness (Tagliazucchi et al. 2016; Tagliazucchi 2017; Toker et al.

2022). Dynamical systems theory in neurosciences has also found a strong paradigm with the concept of manifolds. It's been shown that a high dimensional nonlinear dynamical system can be described in a low dimensional space. This concept was first theoreticized in synergetics (Haken 1983), but restricted to systems living close to a bifurcation, and later generalized to symmetry breaking systems (Pillai et Jirsa 2017). Recent applications of this concept can be found in the domain of motor control (Brennan et Proekt 2019) or to sleep/wake studies (Chaudhuri et al. 2019; Rué-Queralt et al. 2021). The link between dynamics and complexity is still under theoretical exploration (Jirsa et Sheheitli 2022) and, here, we bring an empirical argument in that direction. Indeed, by using a large-scale brain model, we were able to control the dynamical regimes of the network and show that fluidity and responsiveness are maximal within the same parameter range. Fluidity captures the complexity of the manifold (i.e., number of attractors) and responsiveness the complexity upon perturbation. It could be argued that the noise level is not similar in both settings but noise is only present to ensure continuous exploration of the manifold without affecting its topology (Ghosh et al. 2008). Complexity had already been shown to vary across conscious states (Hudetz et al. 2016) and the 1/f slope of the EEG spectrum was also correlated with PCI on the same data we used (Colombo et al. 2019). Our validation results are in line with previous work on spontaneous activity and consciousness. In addition, we demonstrate that it's possible to distinguish ketamine induced unresponsiveness from wakefulness at the individual level with a single metric.

Of important consideration, global coupling is a phenomenological parameter without any biophysical meaning. Several studies have focused on biological mechanisms of consciousness, for instance on the role oscillations in consciousness or the E/I balance. Here, we don't address these questions but rather give a proof of concept that large-scale brain models can help understanding the dynamics related to brain function. We used a model derived from QIF neurons (Montbrió, Pazó, et Roxin 2015) that lacks biological parameters such as ion concentration or synaptic adaptation. Related work has shown that adaptation successfully reproduces dynamical regimes coherent with NREM and wakefulness (Cattani et al 2023) with corresponding realistic PCI values (Goldman et al. 2021). Similarly, using anatomically constrained parameters for brain regions has already been shown to increase the predictive value of brain network models (Wang et. al. Sci Adv 2021, Kong et al. Nat Comm 2022). Nevertheless, we demonstrate that even the symmetry breaking caused by the connectome is sufficient for setting the global working point of the brain, which then links the brain's capacity for generating complex behavior in the different paradigms, that is, rest and stimulation.

One major limitation of our study lies in the algorithm we used to assess complexity in the model. The empirical PCI calculation is done on the average evoked response following stimulation that only lasts a few hundred milliseconds before returning to baseline activity. In the model we spanned this calculation over ten seconds thus capturing a slower dynamic than in real data. Nevertheless, we believe it doesn't affect our statement and in theory the neural mass model we used doesn't have a specific timescale. In future work, some caveats of our work could also be addressed and remedied. First, the imperfect separation of groups for some

of the metrics could be improved by personalized brain modeling. The size of the functional repertoire, for instance, distinguishes wakefulness from anesthesia (including ketamine) but lacks predictive power at the group level. This could be solved using a personalized model including structural information and parameter inference. Second and last, more realistic parameters could be included in the models such as neuromodulatory pathways (Taylor et al. 2022; Kringelbach et al. 2020) to improve explanatory power.

4. Methods:

4.1. Connectome based modeling

The connectome used in this work was obtained from the Human Connectome Project (HCP, (Van Essen et al. 2013)), it was extracted through Diffusion Tensor Imaging (DTI) and belongs to a healthy subject. This connectome captures the tracts weights and lengths between regions of interest (ROI) according to the Desikan Kiliani Atlas (Desikan et al. 2006). In the end 84 cortical and subcortical regions are connected through an undirected graph. Each region of interest (ROI) of the brain was modeled by a neural mass model developed by (Montbrió, Pazó, et Roxin 2015). This model is a derivation of the mean firing rate r and membrane potential V of an all-to-all coupled network of quadratic integrate and fire (QIF) neurons. It is exact in the thermodynamic limit ($N \rightarrow \infty$, with N the number of neurons) and is described by a set of two differential equations:

$$\dot{r} = \frac{\Delta}{\pi} + 2rv$$

$$\dot{v} = v^2 + \bar{\eta} + Jr + I(t) - \pi^2 r^2$$

η is a neuronal excitability parameter that follows a Lorentzian distribution for which the mode $\bar{\eta}$ appears in the mean field equation and Δ is the scale (inter-quartile interval) of the same distribution. Parameter J is the weight of synaptic integration of the QIF neurons. And $I(t)$ is an external current function. All neural masses were constructed equal with parameter values: $\bar{\eta} = -5.0$, $\Delta = 1.0$ and $J = 15.0$. Regions models are connected through their membrane potential by setting:

$$I(t) = G \sum_{m \neq n} W_{nm} r_m (t - \tau_{nm})$$

Where, W_{nm} is the weight (white fiber tract width) and τ_{nm} is the tract length connecting the two regions n and m.

4.2. Data

We retrieved data from studies (Sarasso et al. 2015; Colombo et al. 2019), where 15 healthy subjects between 18 and 28 years old (5 males) were randomly assigned to one of three groups (5 subjects per group) to undergo anesthesia induced by either Xenon, Propofol or Ketamine. For each subject, a 60 channel EEG recorded spontaneous activity of the brain followed by a TMS-EEG session for PCI assessment, once before drug administration (wakefulness) and one under anesthesia. All subjects were unresponsive during anesthesia as measured by the Ramsay scale score 6 (Ramsay et al. 1974). Participants were asked to report

any previous conscious experience upon awakening. Xenon and Propofol anesthesia led to no report of consciousness while Ketamine allowed for retrospective conscious reports (vivid ketamine-dreams). We retrieved the spontaneous EEG recordings for every subject during wakefulness and during anesthesia, as well as the maximum PCI value from the TMS-EEG session and the absence/presence of conscious experience. For more details in the experimental setup and preprocessing steps, see (Sarasso et al. 2015).

4.3. Complexity

4.3.1. Spontaneous complexity

For complexity assessment in spontaneous activity, we calculated the Lempel-Ziv complexity (Lempel et Ziv 1976) denoted as LZ_L on binarized activity. For synthetic data, the bistable nature of the Montbrio model allowed us to binarize firing rate time series (both spontaneous activity and after stimulation) by simple thresholding. The threshold ($r_{thresh} = 0.7$) was determined empirically by visual inspection with the intent to limit false positive and false negative rates of upstate activity. For empirical data, the binarization of spontaneous EEG done after z-scoring each electrode and thresholding at 3 standard deviations.

4.3.2. Perturbational complexity

To capture the complexity of the activity after stimulation we computed an index strongly inspired by the Lempel Ziv version of the perturbational complexity index (Casali et al. 2013). We define the *simulation PCI* ($sPCI$) over a time series of length L as:

$$sPCI = \frac{LZ_L}{C_L}, \text{ with } C_L = \frac{L \times H(L,p)}{log_2 L}$$

where LZ_L is the Lempel-Ziv complexity of a series of length L and c_L is the asymptotic Lempel-Ziv complexity for a random series of the same length L, which is proportional to the source entropy that would have generated the data with the same average activity p. For each $\{G, \sigma\}$ couple, we stimulated a given node $node_i$ at a given time (or trial) t to obtain a $sPCI_{stim}$ value over a window of ten seconds of activity:

$$sPCI_{stim}(node_i, t, G, \sigma) = \frac{LZ_{stim}}{C_{stim}}$$

To distinguish the deterministic response of the system from the spontaneous activity, each of these pci_{stim} value was matched with a baseline value:

$$sPCI_{baseline}(t, G, \sigma) = \frac{LZ_{baseline}}{C_{baseline}}$$

which corresponds to the complexity associated with the spontaneous activity of the realization of the exact same simulation (same parameters, same noise seed) but without the stimulus. The ratio of those two quantities was considered as the change in complexity due to the stimulus:

$$sPCI_{ratio}(node_i, t, G, \sigma) = \frac{sPCI_{stim}(node_i, t, G, \sigma)}{sPCI_{baseline}(t, G, \sigma)}$$

A value of $sPCI_{ratio} > 1$ (respectively $sPCI_{ratio} < 1$) indicates an increase (respectively a decrease) in complexity in response to the stimulus. 17 nodes were randomly selected (for computational limitations) among the 68 cortical nodes and 140 trials were done for each

node near the working point $G \in [0.52, 0.57]$ and $\sigma \in [0.022, 0.039]$, and 6 trials elsewhere. We then selected the maximum $sPCI_{ratio}$ across time and nodes:

$$\max(sPCI_{ratio}(G,\sigma)) = \max_{t,node} sPCI_{ratio}(node_i, t, G, \sigma)$$

Empirical maximum PCI for every participant was provided by (Sarasso et al. 2015) and was also based on Lempel-Ziv complexity. Details about the implementation and calculation can be found in the original publication.

4.4. Fluidity

The extent of the repertoire of functional patterns explored spontaneously by a network is measured by *fluidity* defined as the variance of the upper triangle of the dynamic functional connectivity matrix. A sliding window (of length τ_{win}) of functional connectivity (FC) is applied:

$$FC_{ij}(t) = FC\left[s_i(t'),\ s_j(t')\right]\ with\ t' \in [t - \tfrac{\tau_{win}}{2}\ ; t + \tfrac{\tau_{win}}{2}],$$

$$FC(t) \in R^{N\times N}, \text{ for } N \text{ sources (or electrodes) in the network}$$

This yields a stream of FC matrices across the length of the signal $s(t)$. Dynamic functional connectivity is then computed as the correlation between the upper triangular part of those FC matrices to extract recurrences of functional patterns across time:

$$dFC(t_1, t_2) = corr[UpperTri(FC(t_1)), UpperTri(FC(t_2))]$$

$$dFC \in R^{M\times M}, \text{ for } M \text{ windows}$$

To finish, *fluidity* is the variance of the upper triangle of the dFC matrix, after removal of overlapping windows:

$$fluidity = Var[UpperTri(dFC - B)]$$

$$B_{ij} = \{1\ if\ \left[t_i - \frac{\tau_{win}}{2}\ ; t_i + \frac{\tau_{win}}{2}\right] \cap \left[t_j - \frac{\tau_{win}}{2}\ ; t_j + \frac{\tau_{win}}{2}\right] \neq \emptyset\ \ 0\ otherwise$$

In practice, the diagonal offset to compute *fluidity* is given by the formula:

$$offset = \frac{n_{overlap}}{\tau_{win} - n_{overlap}} + 1$$

With $n_{overlap}$ the number of overlapping time points between two adjacent windows.

In synthetic data functional connectivity was based on the zero-lag Pearson correlation between the firing rate activity of every pair of nodes of the network:

$$FC_{ij}(t) = corr\left[r_i(t'),\ r_j(t')\right]\ with\ t' \in [t - \tfrac{\tau_{win}}{2}\ ; t + \tfrac{\tau_{win}}{2}],$$

In empirical EEG recordings functional connectivity was assessed by the circular correlation coefficient among all pairs of electrodes ($N_{con} = 1770$ for 60 channels) over a sliding window of length τ_{win}. We computed the Hilbert transform of each electrode to extract the instantaneous phase $\varphi_i(t)$ and mean phase $\overline{\varphi_i}$ within each window on a broad ban spectrum (0.5-60Hz). Then between for each pair of electrodes i, j we computed functional connectivity:

$$FC_{ij}(t) = CCorr_{i,j}(t) = \frac{\sum_{t\in\tau_{win}} \sin(\varphi_i(t) - \overline{\varphi_i}) \sin\left(\varphi_j(t) - \overline{\varphi_j}\right)}{\sqrt{\sum_{t\in\tau_{win}} \sin^2(\varphi_i(t) - \overline{\varphi_i}) \sin^2\left(\varphi_j(t) - \overline{\varphi_j}\right)}}$$

4.5. Functional repertoire

To measure the size of the functional repertoire in empirical data we first extracted avalanches on z-scored and binarized EEG recordings (threshold=3s.d). We used a bin size of 1 and verified that branching ratio values were all close to one. The size of the functional repertoire was then defined by the count of unique avalanche configurations during a recording (Sorrentino et al. 2021). In synthetic data, avalanche extraction was not always possible depending on the dynamical regime. We simplified the procedure by counting the number of unique configurations across all time points after binarization.

4.6. Bursting potential

Various modalities have shown that structured brain patterns emerge in short-lived bursts of neuronal activations (Palva et al. 2013; Esfahlani et al. 2020; Beggs et Plenz 2003; Tagliazucchi et al. 2012). To capture these events in our data, we first z-score the data along time, and then perform the root-sum-square (RSS) across electrodes. The RSS profile has values described by a fat-tail distribution and presents a bursting profile characterized by rare sudden jumps. Similar to the PCI, which measures the potential for the system to express complex responses by selecting the maximum of perturbational complexity across an array of stimulations, here we define the potential of spontaneous bursting for the system by selecting the maximum variation of the RSS, which we dub Bursting Potential (BP):

$$BP = \max_{t} grad\,(RSS(t))$$

4.7. Classification

To test for classification accuracy of the resting state metrics we used a Support Vector machine algorithm with a linear kernel. Two different classifiers were evaluated. The first, grouping all participants in the *wakefulness* condition (N=15) against *anesthesia* condition (Ketamine N=5, Xenon N=5, and Propofol N=5). The second, grouping participants in *conscious report* (wakefulness N=15, and Ketamine anesthesia N=5) against *no report* (Xenon N=5, and Propofol N=5 anesthesia). Each classifier was trained using one feature at a time to find the optimal threshold for classification: PCI, fluidity, complexity, size of the functional repertoire, and bursting potential. All features were calculated on the full duration of each recording. Complexity and Functional repertoire features were normalized by the length in minutes.

5. References

1. Attarian, Hrayr P., et Nidhi S. Undevia. 2012. *Atlas of Electroencephalography in Sleep Medicine*. Boston, MA: Springer US. https://doi.org/10.1007/978-1-4614-2293-8.

2. Battaglia, Demian, Thomas Boudou, Enrique C. A. Hansen, Diego Lombardo, Sabrina Chettouf, Andreas Daffertshofer, Anthony R. McIntosh, Joelle Zimmermann, Petra Ritter, et Viktor Jirsa. 2020. « Dynamic Functional Connectivity between Order and Randomness and Its Evolution across the Human Adult Lifespan ». *NeuroImage* 222 (novembre): 117156. https://doi.org/10.1016/j.neuroimage.2020.117156.

3. Beggs, John M. 2008. « The criticality hypothesis: how local cortical networks might optimize information processing ». *Philosophical Transactions of the Royal Society A: Mathematical, Physical and Engineering Sciences* 366 (1864): 329–43. https://doi.org/10.1098/rsta.2007.2092.

4. Beggs, John M., et Dietmar Plenz. 2003. « Neuronal Avalanches in Neocortical Circuits ». *The Journal of Neuroscience* 23 (35): 11167–77. https://doi.org/10.1523/JNEUROSCI.23-35-11167.2003.

5. Brennan, Connor, et Alexander Proekt. 2019. « A Quantitative Model of Conserved Macroscopic Dynamics Predicts Future Motor Commands ». *ELife* 8 (juillet): e46814. https://doi.org/10.7554/eLife.46814.

6. Casali, A. G., O. Gosseries, M. Rosanova, M. Boly, S. Sarasso, K. R. Casali, S. Casarotto, et al. 2013. « A Theoretically Based Index of Consciousness Independent of Sensory Processing and Behavior ». *Science Translational Medicine* 5 (198): 198ra105-198ra105. https://doi.org/10.1126/scitranslmed.3006294.

7. Casarotto, Silvia, Angela Comanducci, Mario Rosanova, Simone Sarasso, Matteo Fecchio, Martino Napolitani, Andrea Pigorini, et al. 2016. « Stratification of Unresponsive Patients by an Independently Validated Index of Brain Complexity ». *Annals of Neurology* 80 (5): 718–29. https://doi.org/10.1002/ana.24779.

8. Chaudhuri, Rishidev, Berk Gerçek, Biraj Pandey, Adrien Peyrache, et Ila Fiete. 2019. « The Intrinsic Attractor Manifold and Population Dynamics of a Canonical Cognitive Circuit across Waking and Sleep ». *Nature Neuroscience* 22 (9): 1512–20. https://doi.org/10.1038/s41593-019-0460-x.

9. Cocchi, Luca, Leonardo L. Gollo, Andrew Zalesky, et Michael Breakspear. 2017. « Criticality in the Brain: A Synthesis of Neurobiology, Models and Cognition ». *Progress in Neurobiology* 158 (novembre): 132–52. https://doi.org/10.1016/j.pneurobio.2017.07.002.

10. Colombo, Michele Angelo, Martino Napolitani, Melanie Boly, Olivia Gosseries, Silvia Casarotto, Mario Rosanova, Jean-Francois Brichant, et al. 2019. « The Spectral Exponent of the Resting EEG Indexes the Presence of Consciousness during Unresponsiveness Induced by Propofol, Xenon, and Ketamine ». *NeuroImage* 189 (avril): 631–44. https://doi.org/10.1016/j.neuroimage.2019.01.024.

11. Damoiseaux, J. S., S. A. R. B. Rombouts, F. Barkhof, P. Scheltens, C. J. Stam, S. M. Smith, et C. F. Beckmann. 2006. « Consistent resting-state networks across healthy subjects ». *Proceedings of the National Academy of Sciences* 103 (37): 13848–53. https://doi.org/10.1073/pnas.0601417103.

12. Deco, Gustavo, Viktor K. Jirsa, Peter A. Robinson, Michael Breakspear, et Karl Friston. 2008. « The Dynamic Brain: From Spiking Neurons to Neural Masses and Cortical Fields ». *PLOS Computational Biology* 4 (8): e1000092. https://doi.org/10.1371/journal.pcbi.1000092.

13. Desikan, Rahul S., Florent Ségonne, Bruce Fischl, Brian T. Quinn, Bradford C. Dickerson, Deborah Blacker, Randy L. Buckner, et al. 2006. « An Automated Labeling System for Subdividing the Human Cerebral Cortex on MRI Scans into Gyral Based Regions of Interest ». *NeuroImage* 31 (3): 968–80. https://doi.org/10.1016/j.neuroimage.2006.01.021.

14. Edlow, Brian L., Jan Claassen, Nicholas D. Schiff, et David M. Greer. 2021. « Recovery from Disorders of Consciousness: Mechanisms, Prognosis and Emerging Therapies ». *Nature Reviews Neurology* 17 (3): 135–56. https://doi.org/10.1038/s41582-020-00428-x.

15. Esfahlani, Farnaz Zamani, Youngheun Jo, Joshua Faskowitz, Lisa Byrge, Daniel P. Kennedy, Olaf Sporns, et Richard F. Betzel. 2020. « High-Amplitude Co-Fluctuations in Cortical Activity Drive Functional Connectivity ». bioRxiv. https://doi.org/10.1101/800045.

16. Fousek, Jan, Giovanni Rabuffo, Kashyap Gudibanda, Hiba Sheheitli, Viktor Jirsa, et Spase Petkoski. 2022. « The Structured Flow on the Brain's Resting State Manifold ». Preprint. Neuroscience. https://doi.org/10.1101/2022.01.03.474841.

17. Fox, Michael, et Michael Greicius. 2010. « Clinical applications of resting state functional connectivity ». *Frontiers in Systems Neuroscience* 4. https://www.frontiersin.org/articles/10.3389/fnsys.2010.00019.

18. Ghosh, Anandamohan, Y. Rho, A. R. McIntosh, R. Kötter, et V. K. Jirsa. 2008. « Noise during Rest Enables the Exploration of the Brain's Dynamic Repertoire ». Édité par Karl J. Friston. *PLoS Computational Biology* 4 (10): e1000196. https://doi.org/10.1371/journal.pcbi.1000196.

19. Giacino, Joseph T., Douglas I. Katz, Nicholas D. Schiff, John Whyte, Eric J. Ashman, Stephen Ashwal, Richard Barbano, et al. 2018. « Practice guideline update recommendations summary: Disorders of consciousness ». *Neurology* 91 (10): 450–60. https://doi.org/10.1212/WNL.0000000000005926.

20. Goldman, Jennifer S., Lionel Kusch, Bahar Hazal Yalçinkaya, Damien Depannemaecker, Trang-Anh E. Nghiem, Viktor Jirsa, et Alain Destexhe. 2021. « A Comprehensive Neural Simulation of Slow-Wave Sleep and Highly Responsive Wakefulness Dynamics ». Preprint. Neuroscience. https://doi.org/10.1101/2021.08.31.458365.

21. Golos, Mathieu, Viktor Jirsa, et Emmanuel Daucé. 2015. « Multistability in Large Scale Models of Brain Activity ». Édité par Christopher J Honey. *PLOS Computational Biology* 11 (12): e1004644. https://doi.org/10.1371/journal.pcbi.1004644.

22. Greicius, Michael. 2008. « Resting-State Functional Connectivity in Neuropsychiatric Disorders ». *Current Opinion in Neurology* 21 (4): 424–30. https://doi.org/10.1097/WCO.0b013e328306f2c5.

23. Haken, Hermann. 1983. *Synergetics: An Introduction*. Vol. 1. Springer Series in Synergetics. Berlin, Heidelberg: Springer. https://doi.org/10.1007/978-3-642-88338-5.

24. Hallett, Mark. 2007. « Transcranial Magnetic Stimulation: A Primer ». *Neuron* 55 (2): 187–99. https://doi.org/10.1016/j.neuron.2007.06.026.

25. Hansen, Enrique C. A., Demian Battaglia, Andreas Spiegler, Gustavo Deco, et Viktor K. Jirsa. 2015. « Functional Connectivity Dynamics: Modeling the Switching Behavior of the Resting State ». *NeuroImage* 105 (janvier): 525–35. https://doi.org/10.1016/j.neuroimage.2014.11.001.

26. Heuvel, Martijn P. van den, et Hilleke E. Hulshoff Pol. 2010. « Exploring the Brain Network: A Review on Resting-State FMRI Functional Connectivity ». *European Neuropsychopharmacology* 20 (8): 519–34. https://doi.org/10.1016/j.euroneuro.2010.03.008.

27. Hobson, J. Allan. 2009. « REM Sleep and Dreaming: Towards a Theory of Protoconsciousness ». *Nature Reviews Neuroscience* 10 (11): 803–13. https://doi.org/10.1038/nrn2716.

28. Hudetz, Anthony G., Xiping Liu, Siveshigan Pillay, Melanie Boly, et Giulio Tononi. 2016. « Propofol Anesthesia Reduces Lempel-Ziv Complexity of Spontaneous Brain Activity in Rats ». *Neuroscience Letters* 628 (août): 132–35. https://doi.org/10.1016/j.neulet.2016.06.017.

29. Jirsa, Viktor, et Hiba Sheheitli. 2022. « Entropy, Free Energy, Symmetry and Dynamics in the Brain ». *Journal of Physics: Complexity* 3 (1): 015007. https://doi.org/10.1088/2632-072X/ac4bec.

30. Kringelbach, Morten L., Josephine Cruzat, Joana Cabral, Gitte Moos Knudsen, Robin Carhart-Harris, Peter C. Whybrow, Nikos K. Logothetis, et Gustavo Deco. 2020. « Dynamic Coupling of Whole-Brain Neuronal and Neurotransmitter Systems ». *Proceedings of the National Academy of Sciences* 117 (17): 9566–76. https://doi.org/10.1073/pnas.1921475117.

31. Lempel, A., et J. Ziv. 1976. « On the Complexity of Finite Sequences ». *IEEE Transactions on Information Theory* 22 (1): 75–81. https://doi.org/10.1109/TIT.1976.1055501.

32. Montbrió, Ernest, Diego Pazó, et Alex Roxin. 2015. « Macroscopic Description for Networks of Spiking Neurons ». *Physical Review X* 5 (2): 021028. https://doi.org/10.1103/PhysRevX.5.021028.

33. Murphy, Michael, Marie-Aurelie Bruno, Brady A. Riedner, Pierre Boveroux, Quentin Noirhomme, Eric C. Landsness, Jean-Francois Brichant, et al. 2011. « Propofol Anesthesia and Sleep: A High-Density EEG Study ». *Sleep* 34 (3): 283–91.

34. O'Byrne, Jordan, et Karim Jerbi. 2022. « How Critical Is Brain Criticality? » *Trends in Neurosciences*, septembre. https://doi.org/10.1016/j.tins.2022.08.007.

35. Palva, J. Matias, Alexander Zhigalov, Jonni Hirvonen, Onerva Korhonen, Klaus Linkenkaer-Hansen, et Satu Palva. 2013. « Neuronal long-range temporal correlations and avalanche dynamics are correlated with behavioral scaling laws ». *Proceedings of the National Academy of Sciences* 110 (9): 3585□90. https://doi.org/10.1073/pnas.1216855110.

36. Patel, Aakash K., Vamsi Reddy, Karlie R. Shumway, et John F. Araujo. 2022. « Physiology, Sleep Stages ». In *StatPearls*. Treasure Island (FL): StatPearls Publishing. http://www.ncbi.nlm.nih.gov/books/NBK526132/.

37. Pillai, Ajay S., et Viktor K. Jirsa. 2017. « Symmetry Breaking in Space-Time Hierarchies Shapes Brain Dynamics and Behavior ». *Neuron* 94 (5): 1010□26. https://doi.org/10.1016/j.neuron.2017.05.013.

38. Pope, Maria, Makoto Fukushima, Richard F. Betzel, et Olaf Sporns. 2021. « Modular origins of high-amplitude cofluctuations in fine-scale functional connectivity dynamics ». *Proceedings of the National Academy of Sciences* 118 (46): e2109380118. https://doi.org/10.1073/pnas.2109380118.

39. Preti, Maria Giulia, Thomas AW Bolton, et Dimitri Van De Ville. 2017. « The Dynamic Functional Connectome: State-of-the-Art and Perspectives ». *NeuroImage*, Functional Architecture of the Brain, 160 (octobre): 41□54. https://doi.org/10.1016/j.neuroimage.2016.12.061.

40. Rabuffo, Giovanni, Jan Fousek, Christophe Bernard, et Viktor Jirsa. 2021. « Neuronal Cascades Shape Whole-Brain Functional Dynamics at Rest ». *Eneuro* 8 (5): ENEURO.0283-21.2021. https://doi.org/10.1523/ENEURO.0283-21.2021.

41. Ramsay, M. A. E., T. M. Savege, B. R. J. Simpson, et R. Goodwin. 1974. « Controlled Sedation with Alphaxalone-Alphadolone ». *BMJ* 2 (5920): 656□59. https://doi.org/10.1136/bmj.2.5920.656.

42. Rué-Queralt, Joan, Angus Stevner, Enzo Tagliazucchi, Helmut Laufs, Morten L. Kringelbach, Gustavo Deco, et Selen Atasoy. 2021. « Decoding Brain States on the Intrinsic Manifold of Human Brain Dynamics across Wakefulness and Sleep ». *Communications Biology* 4 (1): 1□11. https://doi.org/10.1038/s42003-021-02369-7.

43. Sanders, Robert D., Giulio Tononi, Steven Laureys, et Jamie W. Sleigh. 2012. « Unresponsiveness ≠ Unconsciousness ». *Anesthesiology* 116 (4): 946□59. https://doi.org/10.1097/ALN.0b013e318249d0a7.

44. Sanz Leon, Paula, Stuart Knock, M. Woodman, Lia Domide, Jochen Mersmann, Anthony McIntosh, et Viktor Jirsa. 2013. « The Virtual Brain: a simulator of primate brain network dynamics ». *Frontiers in Neuroinformatics* 7. https://www.frontiersin.org/articles/10.3389/fninf.2013.00010.

45. Sarasso, Simone, Melanie Boly, Martino Napolitani, Olivia Gosseries, Vanessa Charland-Verville, Silvia Casarotto, Mario Rosanova, et al. 2015. « Consciousness and Complexity during Unresponsiveness Induced by Propofol, Xenon, and Ketamine ». *Current Biology* 25 (23): 3099–3105. https://doi.org/10.1016/j.cub.2015.10.014.

46. Sarasso, Simone, Adenauer Girardi Casali, Silvia Casarotto, Mario Rosanova, Corrado Sinigaglia, et Marcello Massimini. 2021. « Consciousness and Complexity: A Consilience of Evidence ». *Neuroscience of Consciousness*, août, niab023. https://doi.org/10.1093/nc/niab023.

47. Sorrentino, Pierpaolo, Rosaria Rucco, Fabio Baselice, Rosa De Micco, Alessandro Tessitore, Arjan Hillebrand, Laura Mandolesi, Michael Breakspear, Leonardo L. Gollo, et Giuseppe Sorrentino. 2021. « Flexible Brain Dynamics Underpins Complex Behaviours as Observed in Parkinson's Disease ». *Scientific Reports* 11 (1): 4051. https://doi.org/10.1038/s41598-021-83425-4.

48. Sporns, Olaf. 2011. « The Human Connectome: A Complex Network ». *Annals of the New York Academy of Sciences* 1224 (1): 109–25. https://doi.org/10.1111/j.1749-6632.2010.05888.x.

49. Tagliazucchi, Enzo. 2017. « The Signatures of Conscious Access and Its Phenomenology Are Consistent with Large-Scale Brain Communication at Criticality ». *Consciousness and Cognition* 55 (octobre): 136–47. https://doi.org/10.1016/j.concog.2017.08.008.

50. Tagliazucchi, Enzo, Pablo Balenzuela, Daniel Fraiman, et Dante Chialvo. 2012. « Criticality in Large-Scale Brain fMRI Dynamics Unveiled by a Novel Point Process Analysis ». *Frontiers in Physiology* 3. https://www.frontiersin.org/articles/10.3389/fphys.2012.00015.

51. Tagliazucchi, Enzo, Dante R. Chialvo, Michael Siniatchkin, Enrico Amico, Jean-Francois Brichant, Vincent Bonhomme, Quentin Noirhomme, Helmut Laufs, et Steven Laureys. 2016. « Large-scale signatures of unconsciousness are consistent with a departure from critical dynamics ». *Journal of the Royal Society Interface* 13 (114): 20151027. https://doi.org/10.1098/rsif.2015.1027.

52. Taylor, N. L., A. D'Souza, B. R. Munn, J. Lv, L. Zaborszky, E. J. Müller, G. Wainstein, F. Calamante, et J. M. Shine. 2022. « Structural Connections between the Noradrenergic and Cholinergic System Shape the Dynamics of Functional Brain Networks ». *NeuroImage* 260 (octobre): 119455. https://doi.org/10.1016/j.neuroimage.2022.119455.

53. Toker, Daniel, Ioannis Pappas, Janna D. Lendner, Joel Frohlich, Diego M. Mateos, Suresh Muthukumaraswamy, Robin Carhart-Harris, et al. 2022. « Consciousness is supported by near-critical slow cortical electrodynamics ». *Proceedings of the National Academy of Sciences* 119 (7): e2024455119. https://doi.org/10.1073/pnas.2024455119.

54. Tononi, G. 1998. « Consciousness and Complexity ». *Science* 282 (5395): 1846–51. https://doi.org/10.1126/science.282.5395.1846.

55. Tononi, G., A. R. McIntosh, D. P. Russell, et G. M. Edelman. 1998. « Functional Clustering: Identifying Strongly Interactive Brain Regions in Neuroimaging Data ». *NeuroImage* 7 (2): 133–49. https://doi.org/10.1006/nimg.1997.0313.

56. Van Essen, David C., Stephen M. Smith, Deanna M. Barch, Timothy E.J. Behrens, Essa Yacoub, et Kamil Ugurbil. 2013. « The WU-Minn Human Connectome Project: An Overview ». *NeuroImage* 80 (octobre): 62–79. https://doi.org/10.1016/j.neuroimage.2013.05.041.

57. Xu, Longzhou, Jianfeng Feng, et Lianchun Yu. 2022. « Avalanche Criticality in Individuals, Fluid Intelligence, and Working Memory ». *Human Brain Mapping* 43 (8): 2534–53. https://doi.org/10.1002/hbm.25802.